



Numerical simulations of the flow fields and temperature distribution in a section of a Boeing 767–300 aircraft cabin

Chanfiou Ahmed Mboreha^{a,b,*}, Xavier Tytelman^c, Collins Nwaokocha^{d,*}, Abayomi Layeni^d, Ruth C. Okeze^e, Abdalah Shaibu Amiri^f

^a Key Laboratory of Aircraft Environment Control and Life Support, MIIT, Nanjing University of Aeronautics and Astronautics, Nanjing 210016, PR China

^b College of Aerospace Engineering, Nanjing University of Aeronautics and Astronautics, Nanjing 211106, PR China

^c Starburst Accelerator, 20 Bis Road Balard, 75015 Paris, France

^d Departement of Mechanical Engineering, Olabisi Onabanjo University, Ago-Iwoye, Nigeria

^e Departement of Mechatronics Engineering, Federal Polytechnic, Ilaro, Ogun State, Nigeria

^f Josiah Kibira University College, Bukoba, Tanzania

ARTICLE INFO

Article history:

Received 7 January 2021

Received in revised form 20 May 2021

Accepted 28 June 2021

Available online 10 July 2021

Keywords:

Mixing ventilation system

Displacement ventilation system

Aircraft cabin

CFD

ABSTRACT

In the aircraft cabin, a ventilation system is required to supply pleasant fresh air for a thermally comfortable environment. Mixing and Displacement ventilation systems, are the common mode of air diffusion strategies adopted in the aircraft cabin. However, air movement using these strategies showcased an ease of infection-spread and uneven thermal comfort levels. Hence, the need to develop existing design of air circulation systems for optimized use in aircraft cabins. In this study, we selected two different models of mixing ventilation to study better airflow leading to thermal comfort. The focus of this study is to accurately investigate and study airflow distribution and thermal stability in a cabin space of an aircraft. A Computational Fluid Dynamics (CFD) model is applied to simulate a cabinspace environment inside a Boeing 767–300 airplane at cruise conditions. CFD model was prepared based on an extensive literature survey. Besides, the airflow and thermal stability effect of re-circulation on airborne transmission was also discussed in this paper. A countermeasure design has been proposed, analyzed, and compared with the base model to improve air distribution and thermal stability inside the cabin. By comparing the two models in terms of the distribution of velocity and temperature, this study found that the improved design has more uniform airflow. The results show that the modified design having distributed inlets reduces the path of airflow and may reduce the risk of airborne transmissions such as SARS-CoV-1 (SARS) and the SARS-CoV-2 (Covid-19). In a future further study, we may do with the DPM method to exactly know the effect on airborne transmission.

© 2021 Elsevier Ltd. All rights reserved.

Selection and peer-review under responsibility of the scientific committee of the 3rd International Conference on Computational and Experimental Methods in Mechanical Engineering.

1. Introduction

For some persons, flying is a chance to see other regions and to do so in style, but for others the chance to sit for hours in close proximity to hundreds of other persons is not one that is quite enjoyable. Whatever the viewpoint on this form of transportation, it truly is a new travel spectacle [1]. International Air Transport Association (IATA) statistics have it that about 3.71 billion com-

muters travelled by air in year 2016 [2]; and reported a doubled forecast by 2035, targeting reaching 7.42 billion [3]. Whereas, almost 113,395 flight attendants and 110,500 aircraft engineers, pilots, and co-pilots worked within the cabin space for average man hour of 910 h in 2016 in USA alone. Whereas, to optimize fuel usage of aircraft engine and increase flight corridors, commercial airplane had to change to a cruising altitude close to 13,500 m in the last 40 years. For such altitudes, temperature is close to -56.6°C with a near zero humidity [4,5]. Such ambient condition is dangerous to man except if an environmental control system (ECS) is used for protection [6]. The ventilation system in the aircraft cabin plays a significant role to afford a healthy and conducive environment. The basic functionality of a ventilation system is to

* Corresponding authors at: College of Aerospace Engineering, Nanjing University of Aeronautics and Astronautics, Nanjing 211106, PR China (C. Ahmed Mboreha).

E-mail addresses: chanfiou2017@nuaa.edu.cn (C. Ahmed Mboreha), collinsnwaokocha@gmail.com (C. Nwaokocha).

Nomenclature

ρ	density	G_b	generation of k due to mean buoyancy
x, y, z	index of coordinates	$C_{1\varepsilon}, C_{2\varepsilon}$ and $C_{3\varepsilon}$	constants
μ	dynamic viscosity	Y_M	fluctuating dilatation in compressible turbulence
S	external source term	R	universal gas constant
T	temperature	M_W	molecular weight of the gas
k	kinetic energy of turbulence	P_{op}	operating pressure
ε	dissipation rate of the turbulent kinetic energy		
G_k	generation of k due to mean velocity gradients		

distribute air evenly, diminish cross illness contagion, make a relaxed, harmless and healthy airliner cabin environment. It has been shown that a strong connection between the aircraft cabin ventilation system and airborne transmission of contagious illnesses exists [7]. Hence, enhancing cabin air quality is vital, and to do so, the study on the air circulation in aircraft cabins has drawn considerable attention. A new air delivery system capable of decreasing air mixing on airplanes is of the utmost importance. On top of experimental investigations [8,9], numerous studies have designed the air distribution system in cabin space using CFD. For example, Zhang and Chen [10] applied the RNG k - ε model to study the circulation of CO_2 in a Boeing-767 aircraft cabin. Also, discovered that CO_2 levels with the mixing ventilation system (MVS) were relatively uniform, and the MVS could spread infectious diseases.

Different kinds of ventilation methods were studied to analyze the passenger thermal comfort, along with risk of contagion through the airborne way. Various studies [11–14] demonstrated the influence of ventilation systems on disease spread, air quality, and thermal comfort onboard aircraft. Airlines employ different ventilation strategies for a healthy and comfortable aircraft interior environment. The two widely used ventilation strategies in the aircraft cabin are Mixing and Displacement. In the Mixing Ventilation System (MVS), air typically enters the aircraft cabin from the supply inlets situated closer to the ceiling (under or above the cabin's baggage section, corresponding to the aircraft category) and exits from the exhaust vents placed on the floor on each side of the cabin. In this process, the supplied fresh air mixes with the passenger thermal plumes and contaminated air. The mixing and circulation of fresh air reduce the contaminant concentrations in the aircraft cabin. Although the mixing mode of ventilation is widely employed, yet not effective for efficient energy performance and air quality [15]. Lin et al. [16,17] discovered that general flow pattern in the experimental study was asymmetrical in reference to the cabin cross-section, whose geometry and boundary conditions are symmetrical. Yan et al. [18] applied the reference k - ε model to simulate the air field flow within a full-scale Boeing 767–300 mock-up with un-heated manikins. Authors results validated CFD results in agreement with experimental data such that the two large vortices were fully captured in the simulation. Though different truculent models were evaluated and applied in studying air distribution within a cabin space or an enclosed environment by many researchers [19–22], with majority of the foci not on the evolution of the instantaneous flow field.

Thus, in this study, the evolution of field flow within aircraft cabin model possessing fully occupied heated manikins was simulated with RNG k - ε model turbulence model. Considering the complex flow parameters in the cabin space and the undefined influences of different perturbations in experiments or simulations on the stability of flow fields, yet simulated values were applied to qualitatively compare with the countermeasure design analysis result. Conclusively, due to the limitation available a comparison

is made between two different mesh types and its influence on respective results was studied. The present study utilized computational fluid dynamics to evaluate the airflow in an aircraft cabin equipped with two ventilation modes i.e., the base model (existing mixing ventilation system) and the modified model (the mixing with distributed inlets). The assessment of the two ventilation systems is based on the numerically obtained flow-field pattern, air velocity, and temperature distribution.

2. The mixing and the modified ventilation system descriptions

The geometric model of the aircraft cabin used for the CFD investigation is based on the Boeing 767–300 economy class. A section of 4 rows is considered to create a three-dimensional model using CATIA V5R20 CAD software. Each row comprises 7 seats in a 2–3–2 arrangement. Fig. 1 illustrates the dimensions of the aircraft cabin; the length \times breadth \times height of the cabin is 4.3 m \times 3.3 m \times 2.1 m. The width of the central seat is 1.28 m, whereas the width of the left and right seat is 0.84 m. The width of the aisle is 0.68 m. The cabin was designed with lighting and windows to represent the actual aircraft better. Topp et al. [23] posited that a box-designed manikin is sufficient to investigate the general airflow in the indoor space. Hence, box-designed manikins were utilized to characterize the twenty-eight occupants seated in the aircraft cabin. The passenger breathing zone (when seated) is around 1 to 1.1 m above the floor. The symmetric boundary condition is applied on the rear and front side of the cabin. As the model is symmetric about YZ plane at the center, only half model was used for the analysis, this modeling reduces mesh count and thus computation time with no effect on results. The aircraft cabin model has inlets fixed at the luggage compartment position, supplying fresh air at constant temperature of 292.15 K. The air were exhausted from the outlets on the floor sidewalls.

For this investigation, two separate CAD models are created. The first CAD model is the base model which has one-ceiling inlet provided conditioned air at high velocity, and a floor outlet removed air from the cabin as depicted in Fig. 2-a. The second CAD model is the improved design with distributed inlets at the top of the cabin (one-ceiling inlet and 4 inlets above side walls) as presented in Fig. 2-b. It provides fresh air at high velocity with a constant temperature (292.15 K). The velocity of air is calculated according to the area of inlets and the velocity-inlet boundary condition is assigned to the Inlet. Table 1 classifies the design characteristics of the two ventilation systems.

3. Numerical method

The ease of flexibility, cheap cost, and ease of use, has made computational fluid dynamics (CFD) simulations to be applied by many researchers to investigate the air ventilation system for commercial airplane cabins, was applied in this study to assess the

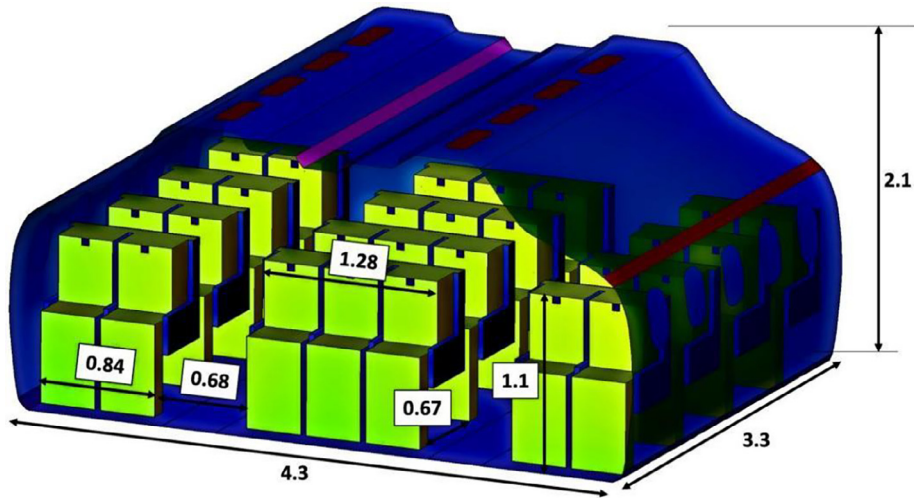


Fig. 1. Dimensions of the Aircraft Cabin, (in meters).

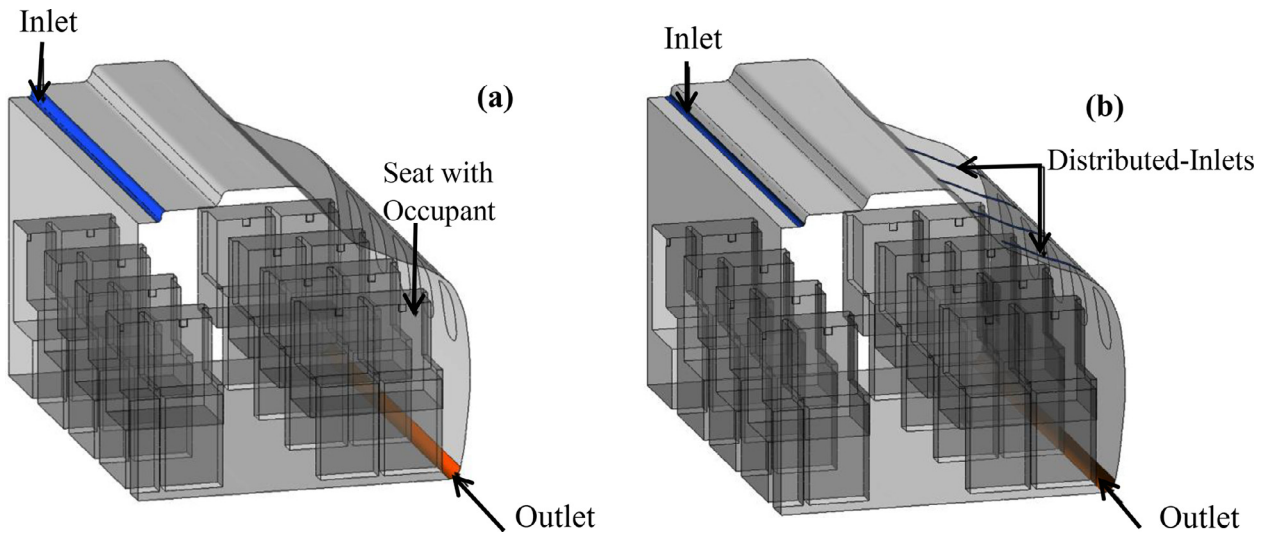


Fig. 2. Aircraft Cabin equipped with: (a) Mixing ventilation system (Base Model-Case-1) and (b) Modified Mixing ventilation system (Case-2).

Table 1
Boundary conditions.

Boundary Type: Velocity Inlet	Boundary	Base Model (Case-1)	Modified model (Case-2)	Units
Supply Air-Velocity	Inlet	0.2	0.2	m/s
Supply Air-Temperature	Inlet	292.15	292.15	K
Supply Air-Water vapor Content	Inlet	0.001008	0.001008	kg of Water vapor/kg of dry air
	Outlet	Outflow		
Boundary Type: Wall	Boundary	Base Model (Case-1)	Modified model (Case-2)	Units
Surface Temperature	Central Deck	298.25		K
	Floor	Adiabatic wall		-
	Passengers	305.15		K
	Lighting	273.25		K
	Seats	Adiabatic wall		-
	Side Wall	290.5		K
Windows	287.15		K	

modified system. The presented numerical approach of the circulation air in the airplane cabin contains resolving a series of Reynolds Averaged Navier Stokes (RANS) equations with various boundary

conditions. The turbulence model adopted in this investigation is RNG k-ε turbulence model. The model provides a more significant presentation for flows demanding recirculation. The modeled

transport equations for turbulence Kinetic Energy (k) and its rate of dissipation (ϵ), are found from the transport equations (1) and (2):

$$\frac{\partial}{\partial t}(\rho k) + \frac{\partial}{\partial x_i}(\rho k u_i) = \frac{\partial}{\partial x_j}(\alpha_k \mu_{eff} \frac{\partial k}{\partial x_j}) + G_k + G_b - \rho \epsilon - Y_M + S_k \quad (1)$$

And

$$\frac{\partial}{\partial t}(\rho \epsilon) + \frac{\partial}{\partial x_i}(\rho \epsilon u_i) = \frac{\partial}{\partial x_j}(\alpha_\epsilon \mu_{eff} \frac{\partial \epsilon}{\partial x_j}) + C_{1\epsilon} \frac{\epsilon}{k} (G_k + C_{3\epsilon} G_b) - C_{2\epsilon} \rho \frac{\epsilon^2}{k} - R_\epsilon + S_\epsilon \quad (2)$$

In equation (1) and (2); $C_{1\epsilon}$, $C_{2\epsilon}$ and $C_{3\epsilon}$ are standards, as in References [24,25], G_k characterizes the development of turbulent kinetic energy (k) as a result of velocity gradients. G_b represents the development of turbulent kinetic energy (k) due to buoyant forces. Y_M characterizes the influence of the changing dilatation in compressible turbulence on the general dissipation rate. σ_ϵ and σ_k are turbulent Prandtl numbers for ϵ and k respectively. S_ϵ and S_k present the user-defined source terms. Pressure based steady-state solver is applied for all the simulations. Flow in the domain is driven due to factors such as gravity forces, the temperature difference in the flow, and the air entering from the ventilation inlets. Different heat sources exist in the domain; for example, passenger body, lighting, ceiling, windows, etc. The temperature changes vary the air density (moving lighter air upward and heavier air downward); this phenomenon causes a recirculation in the flow. This type of flow is called buoyancy driven flow and natural convection. Firstly, gravity was enabled to model buoyancy-driven flows and natural convection, and a magnitude of 9.81 m/s was applied. Secondly, the density in the domain was estimated by using the incompressible ideal gas law. Zhao and Gosselin [26] investigated the modeling assumptions for a numerical simulation of natural ventilation; they showed that the modeling density using incompressible ideal gas law is needed. The solver computed the density as follow:

$$\rho = \frac{P_{op}}{\frac{R}{M_w} T} \quad (3)$$

where, R represents the universal gas constant; M_w represents the molecular weight of the gas and P_{op} represents the operating pressure. It is understood from equation (3) that the density depends on the operating pressure. In the CFD models, pressure at the mid-height of the domain is described as the operating pressure. The pressure-biased solver permits to solve the flow either in a separated or united method. The Pressure-Velocity coupling is achieved using the SIMPLE algorithm. This algorithm uses the relationship existing between the velocity and pressure corrections to derive the pressure field by enforcing mass conservation. A second-order upwind scheme was employed for the spatial discretization of momentum, turbulence, energy, and species transport. Whereas the Pressure interpolation is performed using the Pressure Staggering Option (PRESTO!). All the simulations were performed with a time step size of 0.02 s for more than 10,000-time steps. This corresponds to 200 s of airflow simulations.

4. Results and discussions

To quantitatively examine the performances of the two ventilation systems for the commercial aircraft cabin, this research chose three representative vertical poles within the aircraft cabin space and analyzed the profiles of concerned parameters with height as can be seen in Fig. 3. Pole (P-1) was placed between the back of the seat and passengers (third row/right column), directly in front of the passengers, Pole (P-2) is located in the aisle, while Pole (P-3) was placed between the back of the seat and passengers (third row/middle column). In comparing the obtained results with CFD, two airplanes were considered. One plane (plane-1) is in a

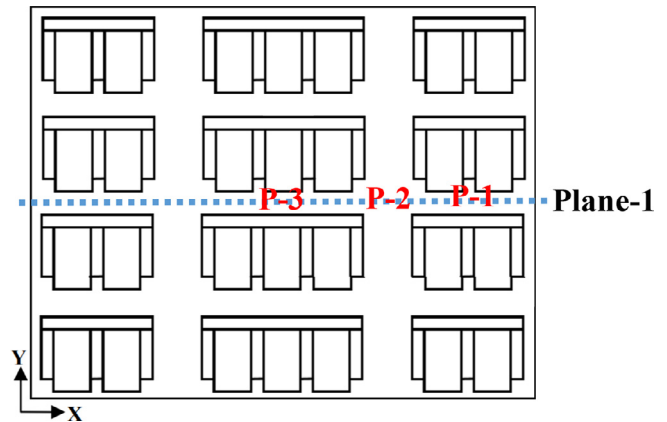


Fig. 3. Two planes and three vertical pole positions where concerned parameters are analyzed.

cross-section across the third seats row, and another plane (plane-2) is a longitudinal plane as presented in Fig. 3. These planes are utilized to show the contours for the air velocity and temperature distribution.

4.1. Velocity and temperature distribution

Fig. 4 and Fig. 5, illustrated the velocity and temperature distribution on the lateral cut-section plane (Plane-1). The vector plot is used to analyze the direction of airflow, and the contours are used to determine the magnitude of air velocity (m/s) and temperature (K). The Base model (Case-1) has ceiling inlets and modified model (Case-2) has distributed inlets. In the Base model (Case-1), the primary air enters the cabin space from the two-ceiling inlets at a velocity of 0.2 m/s. The inlets direct the supplied air towards the left and right passengers. The supplied air-jet flows through the aisle to impinge the passengers, enter the leg-room space, and eventually reach the floor surface.

The air velocity near the floor surface ranges from 0.04 m/s to 0.13 m/s. From the floor surface, the primary air separates in two paths to become the secondary air. The first path is towards the cabin side-wall, in this path, the air flows along the floor surface, and exits from the outlet located close to the floor. In the second path, the air enters the central seat legroom space and rises upward with the thermal plumes (of the center passengers) at a velocity of 0.08 m/s. This secondary air flows upward, reaches the ceiling, and reflects down with the primary inlet air to form a large circulation region as can be seen in Figure. The Fig. 6, represents the velocity distribution along Z direction. The graphs clearly presented the velocity deviation for the modified model (Case-2) has having less value on all poles than the base model (Case-1).

The velocity is distributed more uniformly in the cabin with the distributed inlets (Case-2). Temperature contour for the base model (Case-1) is presented in Fig. 5-a, which illustrates a uniform temperature of 300.2 K within the passenger’s breathing zone. The temperature differential between the supplied air and the air near the floor is less than 3 K. Few regions of high-temperature air (i.e., 304 K) exist due to the presence of cabin lights and passenger thermal plumes near the sidewall, side deck, and center ceiling spaces.

The cabin with modified model (Case-2) employed the mixing type of ventilation for the global airflow, therefore the global airflow movement for the cabin with the modified model is at par with that of the cabin equipped with the mixing ventilation system. Hence, the velocity vectors (in Fig. 7) showcase air flow movement identical to that of the base model (Case-1) with a small

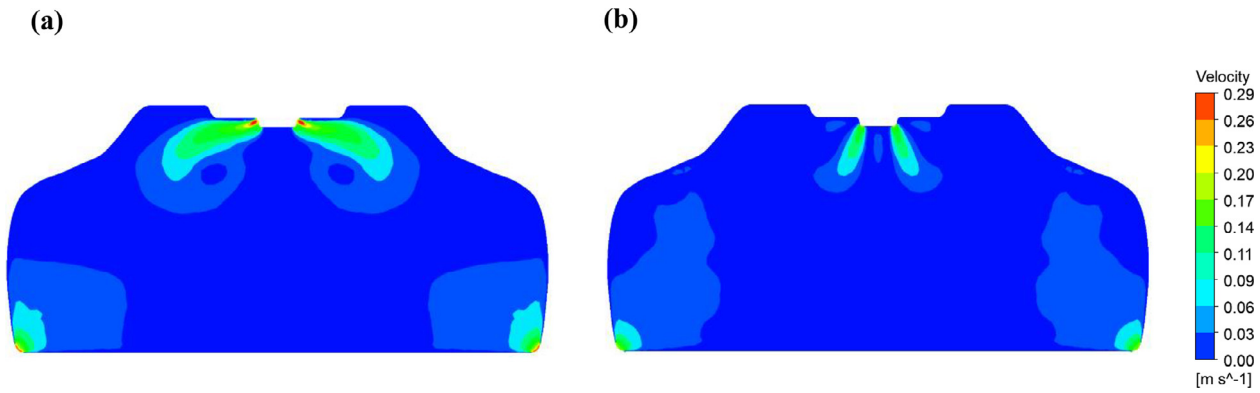


Fig. 4. The Velocity contours on plane1 (Z = 1.71 m): (a) Base Model and (b) Modified model.

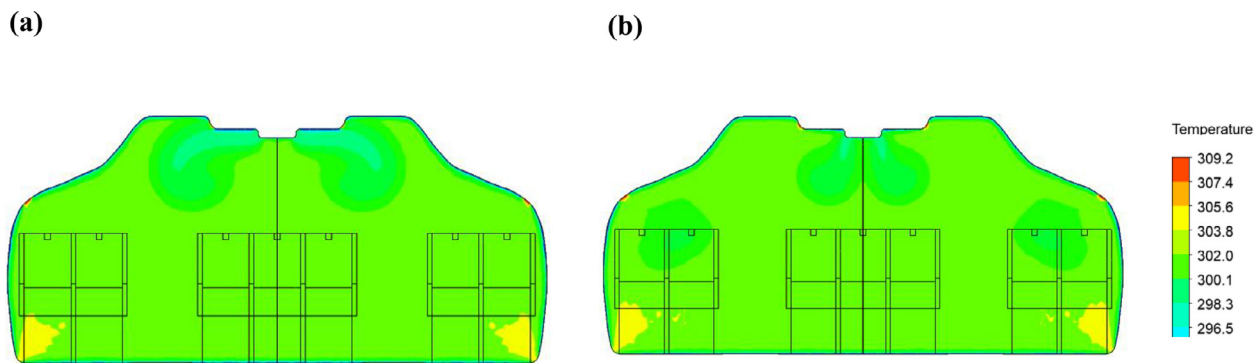


Fig. 5. The Temperature contours on plane1 (Z = 1.71 m) : (a) Base Model and (b) Modified model.

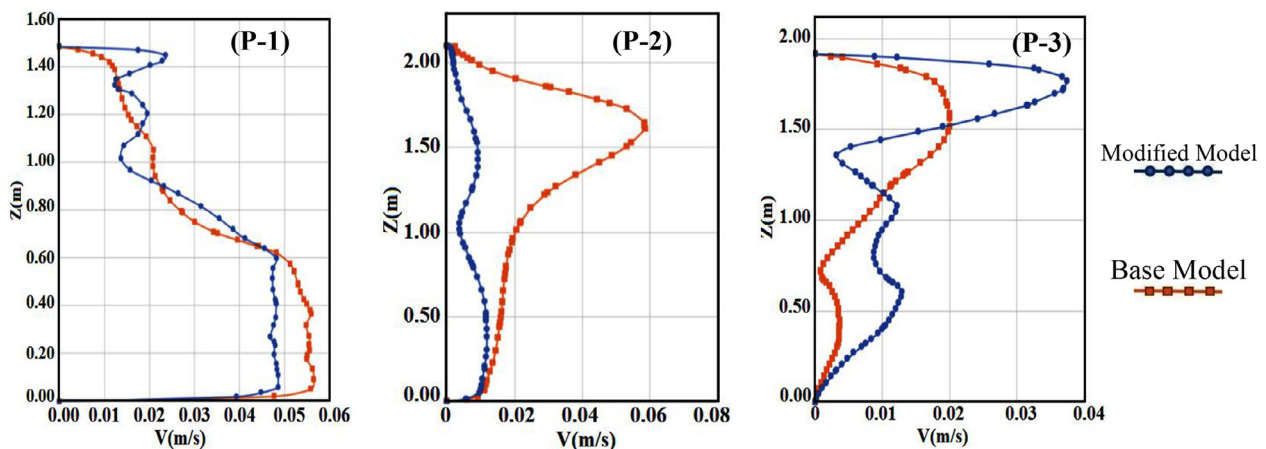


Fig. 6. Velocity profiles on the three different poles in the aircraft cabin.

circulation region than Case-1. The velocity contour (Fig. 4) reveals that there is symmetry in the air velocity. The supply air temperature is 298 K, however in the breathing level on the right and left columns, due to the presence of distributed-inlets, the temperature of the air is 295 K.

In the base model (Case-1), the air has an upward movement around the central passengers as can be seen in Fig. 8-a. This upward movement of air is due to the reflection of primary air from the floor surface. The reflected air, in combination with the passenger-thermal plumes, rises upward to the ceiling. The narrow gap between the seats (legroom) increased the velocity of air to 0.1 m/s. The rest of the regions showcases an air velocity ranging

from 0.01 m/s to 0.05 m/s. The temperature distribution (Fig. 9-a) from the floor to the passenger’s face is not very uniform, however, the presence of thermal plumes and cabin lights raised the temperature of the air near the ceiling, the vertical difference observed on this plane is less than 3 K. The Fig. 10, represents the temperature distribution along Z direction. At pole-2 the modified model (Case-2) has more uniform temperature distribution at pole-2 than the base model (Case-1). while, the base model (Case-1) had a uniform temperature distribution at pole-1 and pole-3.

The velocity of the air supplied from the distributed-inlet is 0.16 m/s. The rest of the cut-section showcases a velocity ranging from 0.01 m/s to 0.07 m/s as presented in Fig. 8-b. In the modified

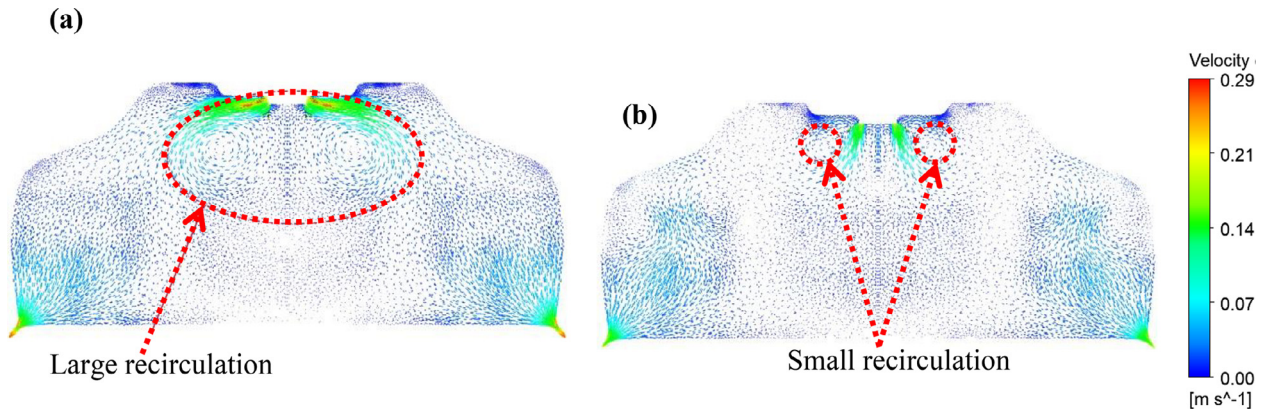


Fig. 7. The Velocity vectors on plane1 (Z = 1.71 m): (a) Base Model and (b) Modified model.

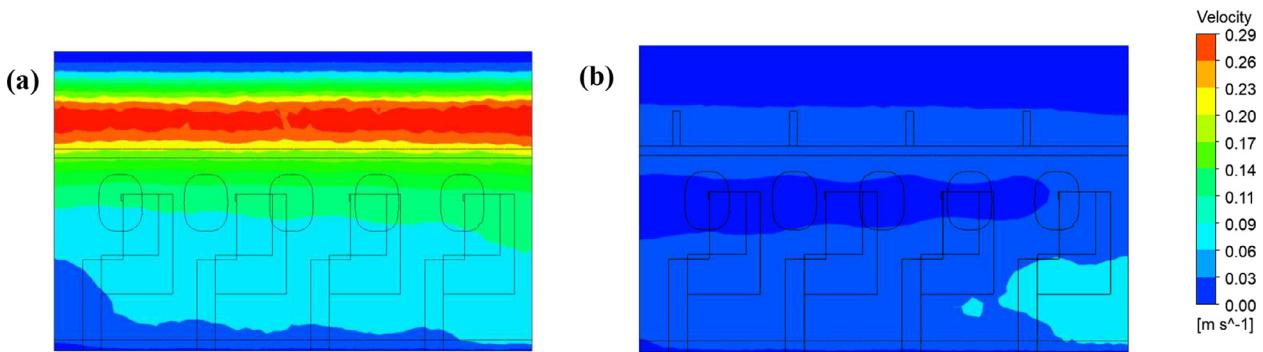


Fig. 8. The Velocity contours on plane-2(X = 3.28 m): (a) Base Model and (b) Modified model.

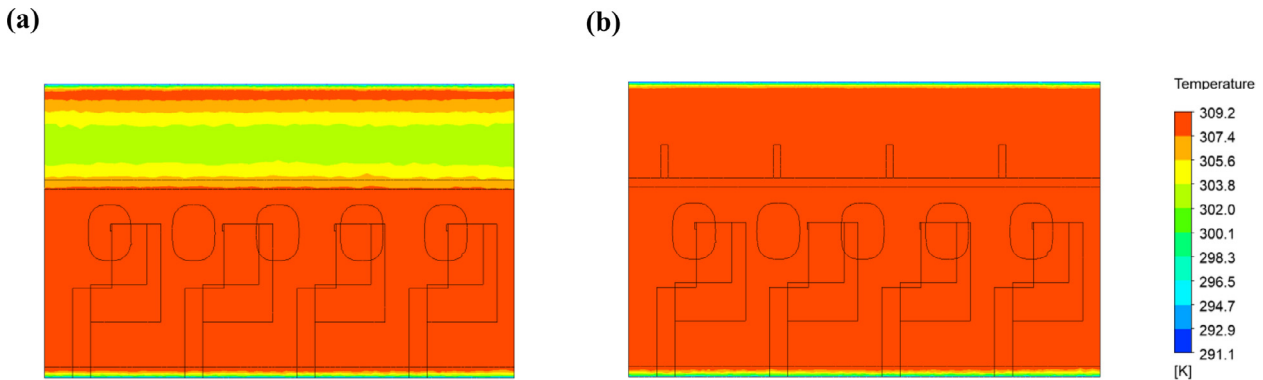


Fig. 9. The Temperature contours on plane-2 (X = 3.28 m): (a) Base Model and (b) Modified model.

model (Case-2), the upperwall, on which the distributed inlets are mounted, has restricted the movement of the thermal plume from the passenger side body. Therefore, in this case, the path of the thermal plume is from the front of the passenger body. Hence, the temperature contour showcases a strong intensity of thermal plume in comparison with the other the base model (Case-1). The temperature distribution (Fig. 9-b) from the floor to the passenger's face was uniform. The RNG k-ε turbulence model has been proved to be capable enough to simulate the cabin airflow [27]. In this study the velocity contours plotted on vertical plane-1, shown that the field flow simulated by the RNG k-ε turbulence model is stable and symmetric in both cases. The area is calculated in this study on plane-1, where the velocity is less than or equal to

0.1 m/sec. The base model (Case-1) had 4.04 m² and the modified model (Case-2) had 4.12 m². It shows that the velocity variation is less in the modified model (Case-2) and more uniform velocity distribution than in the base model (Case-1).

Lin et al. [17] noticed swing movements across the symmetric plane in B767-300 aircraft cabin space. In this study, a swing motion across symmetric plane around aisle region is also observed as shown in Figure G. Zhang [11] explained that thermal discomfort is not a problem, as long as temperature difference is less than 3 K. In this study, temperature difference is not more than 3 K. Hence, both the ventilation systems, i.e., base and modified models showcased air velocity and temperature ranges under the allowable limits specified by ASHRAE [28].

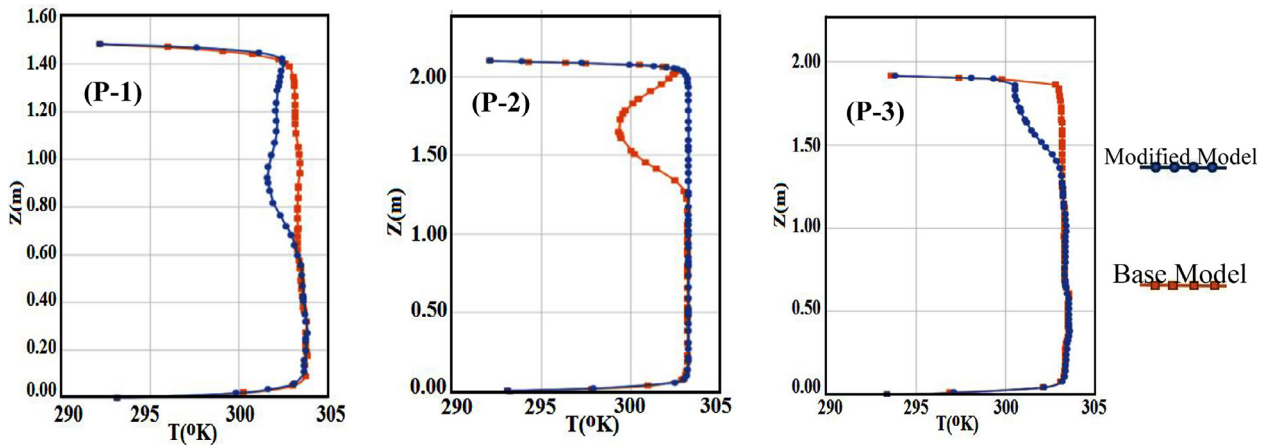


Fig. 10. Temperature profiles on the three different poles in the aircraft cabin.

4.2. Effect of grid type on results

In the present study, authors studied the effect of Grid type on computing cost and the accuracy of numerical simulation on aircraft cabin. Since Polyhedral mesh was rarely used in aircraft cabin simulation and due to the limitation of space in this paper, this study considered only the tetrahedral mesh having 2.78 M elements and polyhedral mesh having 0.54 M mesh count for the comparison. A tetrahedron shape possesses 6 edges and 4 vertices, and is surrounded with four triangular faces [29]–[30]. The polyhedral mesh is gotten directly from the tetrahedral mesh by forming polygons about individual node in the tetrahedral mesh [31], Polyhedral mesh presents very efficient results in large number of simulations. The Fig. 11, shown the grid distributions of the two different mesh types.

The Fig. 12, shown different velocity profiles obtained at three different poles with polyhedral mesh and tetrahedral mesh. Results for both mesh types reveal similar patterns at the poles and the numerical results also nearly similar for tetrahedral and polyhedral mesh type. Time taken for simulation of polyhedral mesh was 1/4 of the tetrahedral mesh. We remarked that using the polyhedral mesh may reduce a computing time with good con-

versions. Hence the polyhedral mesh is comparatively good than the tetrahedral mesh in aircraft cabin simulations.

4.3. Future studies

The results show that the modified design having distributed inlets reduced the path of airflow and may reduce the risk of airborne transmissions such as SARS-CoV-1 (SARS) and the SARS-CoV-2 (Covid-19). The future study shall investigate the following characteristics to demonstrate the modified model (Case-2) to be an efficient ventilation system.

- The spread of passenger emitted carbon dioxide in the aircraft cabin: A comparison of the based model (Case-1) and the modified model (Case-2) based on the concentrations of carbon dioxide will illustrate the efficiency of the modified model (Case-2) in reducing carbon dioxide levels.
- Contaminant Particle Transport: Assigning a random passenger to be sick (index passenger) and analyzing the spread of contaminant particles emitted through cough/sneeze.

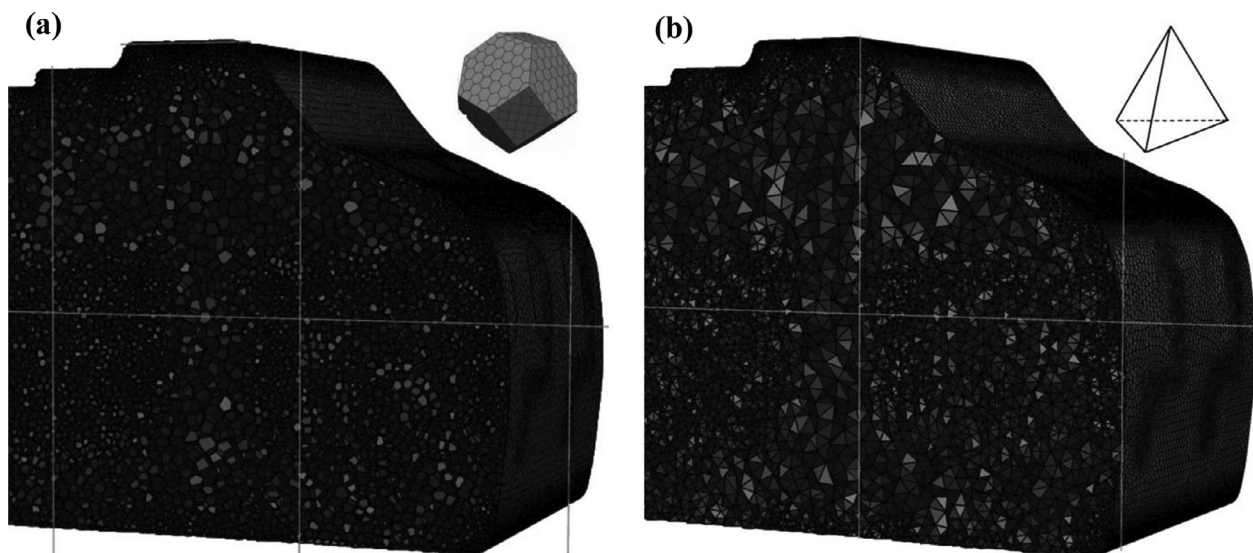


Fig. 11. Grid distributions: (a) Polyhedral Mesh and (b) Tetrahedral Mesh.

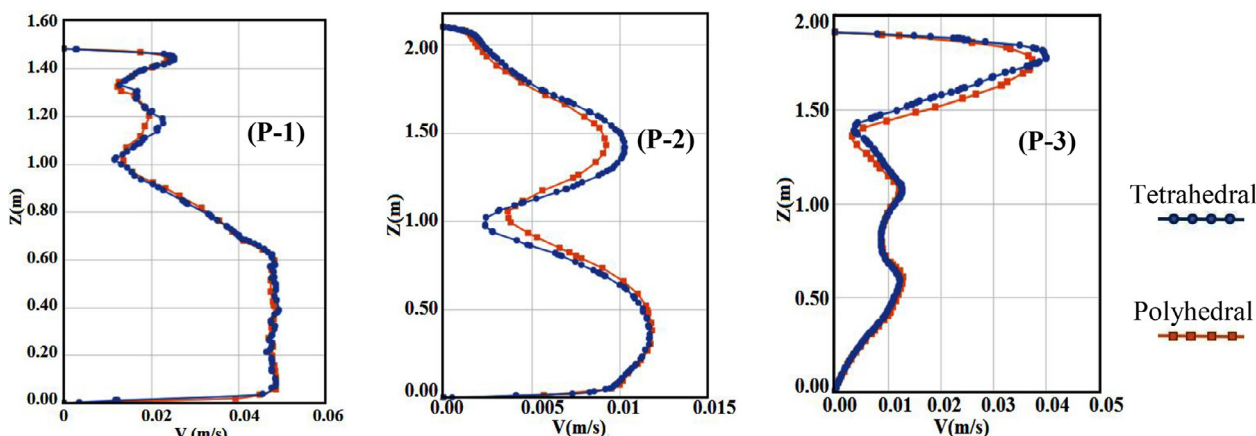


Fig. 12. Comparison of the Velocity profiles with two different grids.

5. Conclusions

In the last decade, flow and thermal analysis of airplane cabins has been studied using experimental and numerical data. Three methods are available for aircraft ventilation such as mixing, displacement, and personalized ventilation. The Mixing ventilation has good airflow and thermal comfort but it is insignificant in airborne disease transport. In the present study, the authors are numerically investigating two different models of mixing ventilation to study better the air quality, thermal comfort, and the risk of airborne diseases. The conclusions were as follows:

The Results showed that the ventilation system with distributed inlets has uniform flow distribution inside the aircraft cabin.

As temperature difference found not more than 3 K, so both designs are considered to have good performance. While the overall temperature for the modified design (with distributed inlets) was found less than the base model, the distributed inlets improved the cooling rate.

To reduce airborne transmission, path transfer by air should be minimum and re-circulation should be less. In this study, the ventilation system with distributed inlets could also decrease the spread of airborne disease as it had less re-circulation zone.

Hence, based on these results, it is suggested that the proposed model with the distributed inlets be possibly more beneficial for the upcoming airline.

Declaration of Competing Interest

The authors declare that they have no known competing financial interests or personal relationships that could have appeared to influence the work reported in this paper.

Acknowledgment

The authors are grateful to their colleagues and teammates for their helpful suggestions.

References

- [1] C. Said, C. Ahmed, G. Kumar, and A. Layenil, "Staying Healthy On Long-Haul Commercial Flights: Guidelines," vol. 2, no. 7, pp. 510–515, 2020, doi: 10.35629/5252-0207510515.
- [2] International Air Transport Association (IATA), "Another Strong Year for Air Travel in 2016," IATA Press Release No.: 5, 2017.

- [3] IATA, "IATA Forecasts Passenger Demand to Double Over 20 Years," IATA Press Release No.: 59, 2016.
- [4] E.H. Hunt, D.H. Reid, D.R. Space, F.E. Tilton, Commercial airliner environmental control system, Proc. Aerosp. Med. Assoc. Annu. Meet, Anaheim USA, 1995.
- [5] "ABSTRACTS. (1974). SAE Transactions, 83, 41–191. Retrieved December 14, 2020, from <http://www.jstor.org/stable/44434089>."
- [6] N. R. C. (US) C. on A. Q. in P. C. of C. Aircraft, "The Airliner Cabin Environment and the Health of Passengers and Crew," Natl. Acad. Press (US), 2002.
- [7] Y. Li, G.M. Leung, J.W. Tang, X. Yang, C.Y.H. Chao, J.Z. Lin, J.W. Lu, P.V. Nielsen, J. Niu, H. Qian, A.C. Sleight, H.-J.-J. Su, J. Sundell, T.W. Wong, P.L. Yuen, Role of ventilation in airborne transmission of infectious agents in the built environment - A multidisciplinary systematic review, *Indoor Air*. 17 (1) (2007) 2–18, <https://doi.org/10.1111/ina.2007.17.issue-110.1111/j.1600-0668.2006.00445.x>.
- [8] R. You, J. Chen, Z. Shi, W. Liu, C.-H. Lin, D. Wei, Q. Chen, Experimental and numerical study of airflow distribution in an aircraft cabin mock-up with a gasper on, *J. Build. Perform. Simul.* 9 (5) (2016) 555–566, <https://doi.org/10.1080/19401493.2015.1126762>.
- [9] Z. Zhang, X. Chen, S. Mazumdar, T. Zhang, Q. Chen, Experimental and numerical investigation of airflow and contaminant transport in an airliner cabin mockup, *Build. Environ.* 44 (1) (2009) 85–94, <https://doi.org/10.1016/j.buildenv.2008.01.012>.
- [10] T. Zhang and Q. (Yan) Chen, "Novel air distribution systems for commercial aircraft cabins," *Build. Environ.*, vol. 42, no. 4, pp. 1675–1684, 2007, doi: 10.1016/j.buildenv.2006.02.014.
- [11] T. Zhang, Q. Chen, Comparison of different ventilation systems for commercial aircraft cabins, *Proc. indoor air 4 (2002)* 3205–3210.
- [12] R. G. and H. N. N. Abhishek Raina, Logeshkumar Srinivasan Venkatesan, J. Schminder, "CFD Study of Different Aircraft Cabin Ventilation Systems on Thermal Comfort and Airborne Contaminant Transport," Linköping Univ., 2020.
- [13] B. W. J. Michael D. Anderson, Mohammad H. Hosni, "Effect of gaspers on airflow patterns and the transmission of airborne contaminants within an aircraft cabin environment," KANSAS STATE Univ. Manhattan, Kansas, 2012.
- [14] C.A. Mboreha, S. V. G. Kumar, C. Nwaokocha, A. Layenil, Comparative study of mixing and under-flow air distribution system in an aircraft cabin using CFD, *Int. J. Res. Eng. Innov.* 4 (5) (2020) 280–286, <https://doi.org/10.36037/IJREI10.36037/IJREI.202010.36037/IJREI.2020.4507>.
- [15] T. Karimipannah, H.B. Awbi, B. Moshfegh, The Air Distribution Index as an Indicator for Energy Consumption and Performance of Ventilation Systems, *J. Human-Environment Syst.* 11 (2) (2008) 77–84, <https://doi.org/10.1618/jhes.11.77>.
- [16] C. H. Lin et al., "Numerical simulation of airflow and airborne pathogen transport in aircraft cabins - Part I: Numerical simulation of the flow field," 2005.
- [17] C. H. Lin et al., "Numerical simulation of airflow and airborne pathogen transport in aircraft cabins - Part II: Numerical simulation of airborne pathogen transport," 2005.
- [18] W. Yan, Y. Zhang, Y. Sun, D. Li, Experimental and CFD study of unsteady airborne pollutant transport within an aircraft cabin mock-up, *Build. Environ.* 44 (1) (2009) 34–43, <https://doi.org/10.1016/j.buildenv.2008.01.010>.
- [19] W. Liu, J. Wen, C.-H. Lin, J. Liu, Z. Long, Q. Chen, Evaluation of various categories of turbulence models for predicting air distribution in an airliner cabin, *Build. Environ.* 65 (2013) 118–131, <https://doi.org/10.1016/j.buildenv.2013.03.018>.
- [20] Z. Zhai, Z. Hang, and Q. Zhang, WeiChen, "Evaluation of Various Turbulence Model in Predicting Airflow and Turbulence in Enclosed Environments by CFD Part 1: Summary of Prevalent Turbulence Models," HVAC&R Res., 2012.
- [21] Z. Zhang, W. Zhang, Z.J. Zhai, Q.Y. Chen, Evaluation of various turbulence models in predicting airflow and turbulence in enclosed environments by CFD: Part 2—comparison with experimental data from literature, *HVAC R Res.* 13 (6) (2007) 871–886, <https://doi.org/10.1080/10789669.2007.10391460>.

- [22] Z. Feng, Z. Long, Q. Chen, Assessment of various CFD models for predicting airflow and pressure drop through pleated filter system, *Build. Environ.* 75 (2014) 132–141, <https://doi.org/10.1016/j.buildenv.2014.01.022>.
- [23] C. Topp, P. V. Nielsen, and D. N. Sørensen, "Application of computer simulated persons in indoor environmental modeling," 2002.
- [24] B.E. Launder, D.B. Spalding, *Lectures in Mathematical Models of Turbulence*. (1972).
- [25] R.A.W.M. Henkes, F.F. Van Der Vlugt, C.J. Hoogendoorn, Natural-convection flow in a square cavity calculated with low-Reynolds-number turbulence models, *Int. J. Heat Mass Transf.* 34 (2) (1991) 377–388, [https://doi.org/10.1016/0017-9310\(91\)90258-C](https://doi.org/10.1016/0017-9310(91)90258-C).
- [26] R. Zhao and L. Gosselin, "Natural Ventilation of a Tall Industrial Building : Investigation on the Impact of Modeling Assumptions," 2014.
- [27] C. Yang, X. Zhang, X. Cao, J. Liu, and F. He, "Numerical Simulations of the Instantaneous Flow Fields in a Generic Aircraft Cabin with Various Categories Turbulence Models," 2015, doi: 10.1016/j.proeng.2015.09.163.
- [28] ASHRAE, Standard 55-2013 - Thermal Environmental Conditions for Human Occupancy. 2013.
- [29] J. Pellerin, A. Johnen, K. Verhetsel, J.-F. Remacle, Identifying combinations of tetrahedra into hexahedra: A vertex based strategy, *CAD Comput. Aided Des.* 105 (2018) 1–10, <https://doi.org/10.1016/j.cad.2018.05.004>.
- [30] M. Sosnowski, J. Krzywanski, K. Grabowska, and R. Gnatowska, "Polyhedral meshing in numerical analysis of conjugate heat transfer," 2018, doi: 10.1051/epjconf/201817002096.
- [31] R.V. Garimella, J. Kim, M. Berndt, in: *Proceedings of the 22nd International Meshing Roundtable*, Springer International Publishing, Cham, 2014, pp. 313–330, https://doi.org/10.1007/978-3-319-02335-9_18.